# Impact of Front- and Rear Stage High Pressure Compressor Deterioration on Jet Engine Performance

Gerald Reitz and Jens Friedrichs[1]

ISROMAC 2017

International Symposium on Transport Phenomena and Dynamics of Rotating Machinery

Maui, Hawaii

December 16-21, 2017

**Abstract**

Current civil aviation is characterized by rising cost and competitive pressure, which is partly passed to the MRO (Maintenance, Repair and Overhaul) companies. To improve the maintenance, the condition based maintenance is established, which is characterized by tailored maintenance actions for each part of the jet engine, depending on the individual engine history and operating conditions. Thereby, prediction models help the engineers to authorize maintenance actions as effective as possible. This paper will help to improve these prediction models. Therefore, the influence of specific deterioration of high pressure compressor (HPC) to jet engine performance parameters like exhaust gas temperature (EGT) and specific fuel consumption (SFC) will be investigated. For this purpose, computational fluid dynamic (CFD) calculations of deteriorated HPC geometries are carried out and serve as basis to scale the reference HPC performance characteristics to deteriorated ones. To evaluate the changes in performance parameters, a modular performance synthesis model is set up. In this model, the HPC map is exchanged by deteriorated ones. As a result, the influence of geometric deviations to the design intent can be determined and the MRO is able to focus on the most relevant sections of the compressor blading.

**Keywords**

Compressor deterioration — Engine performance — Condition based maintenance

[1] *Institute of Jet Propulsion and Turbomachinery, Technische Universität Braunschweig, Braunschweig, Germany*

***Corresponding author**: g.reitz@ifas.tu-braunschweig.de

## INTRODUCTION

During operation of a jet engine deterioration occurs and is continually reducing the engine performance. As a result, the SFC and EGT are increasing with on-wing time of the engine, which also leads to an increase in direct operating costs (DOC). Is the EGT reaching a given limit, the engine has to be removed from the airplane and to be overhauled by a MRO company. For a long time the time-based maintenance was standard procedure to repair an engine. Thereby, no special attention to the operational- and maintenance history is given and the engine components receive more or less standard repairs. Nowadays, the time based maintenance gets replaced by the condition based maintenance. The condition based maintenance is characterized by the requirement of a detailed prediction and examination of the engine components and its piece parts at the incoming inspection of the overhaul and tailored maintenance actions, depending on the engine history and condition.

For further improvement of the condition based maintenance, the influence of each engine component and its piece parts to the engine performance needs to be known. Using the example of the HPC, the aerodynamics of its individual blading has to be determined to predict the changes of the resulting compressor map. Thus, the MRO would be able to repair and rearrange the blading in such a way that the costumers demands for the planned next operation are met as cost-effective as possible, while respecting the given limits of the Engine Manual (EM).

In order to determine the geometric variances of deteriorated HPC airfoils, a multitude of HPC airfoils has been digitized. This paper focuses on modified front- and rear stages of the HPC. Therefore, more than two complete rotor bladings of operated jet engines [1] and additionally 40 stator vanes for each of the analyzed HPC-stages have been digitized by a structured light 3D-scanner in conjunction with a photogrammetric system. To determine manufacturing tolerances, 30 new airfoils of each analyzed compressor row have been digitized, too. Afterwards, the airfoils have been analyzed with respect to their geometric parameters by an in-house programmed algorithm [2]. Subsequently, aerodynamic sensitivities of the geometric properties have been investigated using CFD-methods. Therefore, extensive Design of Experiments (DoE) for the front and rear stage have been carried out [3] [4]. To reduce the number of independent geometric properties, the geometric parameters have previously been scanned for possible correlations [5].

This paper takes the next step of this field of research and is focusing on the changes of the jet engine performance due to compressor deterioration. Therefore, a modular performance synthesis model of a popular

two-shaft bypass jet engine was set up and validated by test cell data. To analyze the impact of deteriorated HPC-bladings, the geometric parameters of a front- and rear stage of the HPC are modified and implemented in a full HPC-model. Thereby, the results of the previous DoEs [3] [4] were used to change the geometric parameters of the regarded compressor stages to achieve stage setups with low and high stage efficiency. The aerodynamics of the HPC is simulated using methods of CFD. With the deteriorated throttle lines, the reference HPC-map is scaled and implemented in the performance model of the jet engine. Thus, it is possible to identify the more relevant HPC-stage, to predict the possible performance range by repairing the stage and to analyze the interactions between the engine components.

## GENERATION OF DETERIORATED STAGE SETUPS

To determine the aerodynamic sensitivities to the geometric parameters of the regarded compressor stages, two extensive DoEs were done [3] [4]. Therefore, the geometric properties of the rotor blades and stator vanes have been modified in a range of $\pm 1.5\sigma$ (standard deviation of the deteriorated airfoils) around the new part mean value. The used standard deviation of the geometric properties was calculated by analyzing a high number of digitized flown airfoils [1]. The throttle lines of the modified stage geometries were simulated by methods of CFD. Afterwards, these throttle lines have been analyzed at a reference mass flow. The aerodynamic results like efficiency and pressure rise were used in conjunction with the corresponding geometric values to train a meta-model using the *Kriging-Method* [6]. After validating the prediction quality of the meta-model, the user is able to predict the aerodynamic performance of unknown geometric variations without using further CFD calculations.

### Front stage sensitivities

Using the trained meta-models, *Pareto* charts were used to identify the aerodynamic sensitivities to the geometric parameters. Therefore, all geometric properties were changed independently about $\pm\sigma$ and the aerodynamic performance parameters were calculated by the meta-model. The aerodynamic changes for one performance parameter, influenced independently by all geometric properties successively, were summed and plotted in a *Pareto* chart. Fig. 1 shows the *Pareto* chart for the isentropic efficiency $\eta_{is}$ of the front stage, analyzed at the reference mass flow. As can be seen, the most relevant geometric parameters are the leading edge thickness of the stator vane $V\ t_{LE}$, the max. camber of the rotor blade $B\ C_{max}$ and the leading edge thickness of the rotor blade $B\ t_{LE}$. The accumulated impact of the three most important parameters is almost the half of the overall changes caused by 22 geometric properties.

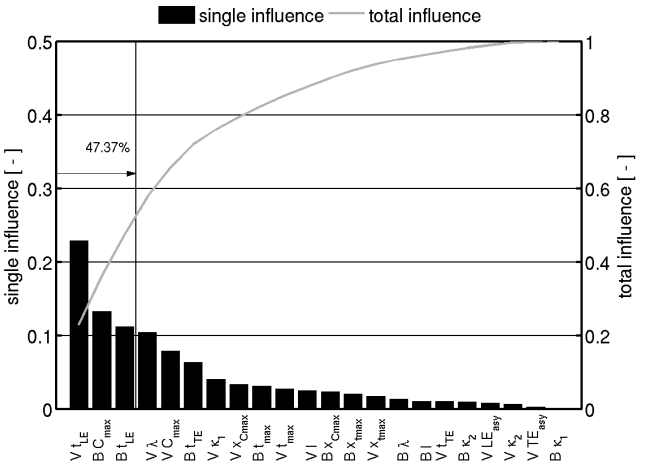


**Figure 1.** *Pareto* chart of isentropic efficiency $\eta_{is}$ at the front stage

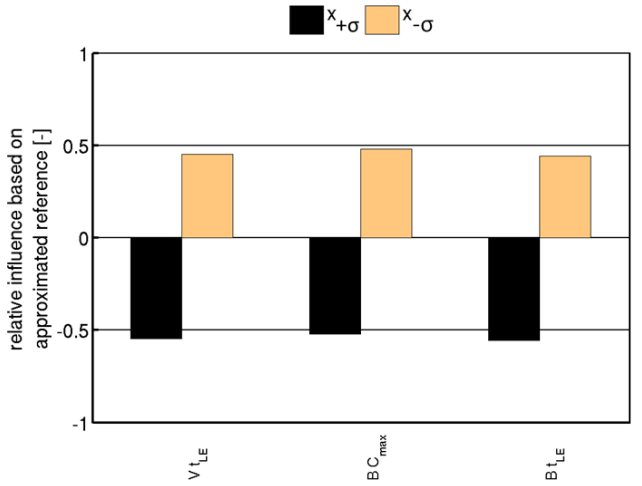


**Figure 2.** Sensitivies of $\eta_{is}$ to geometric changes at the front stage

A closer look to the three dominating geometric properties is given in Fig. 2. Here, the direction of the aerodynamic performance parameter changes caused by the geometric variations is shown. Black bars are indicating an increased geometric property by $\sigma$ and orange ones decreased values of the same amount. Thus, the geometric parameters are varied symmetrically around the reference value and an equal change of the isentropic efficiency $\eta_{is}$ would be expected. Thereby, bars above zero are indicating an increased value for the isentropic efficiency $\eta_{is}$ and vice versa. Please take note, that this illustration is just visualizing the directional dependency and its sensitivity of the isentropic efficiency $\eta_{is}$ towards the geometric property and not the magnitude of change. For the front stage the isentropic efficiency $\eta_{is}$ is increasing with decreased leading edge thicknesses of the rotor blade $B\ t_{LE}$ and stator vane $V\ t_{LE}$ and with decreased max. profile camber of the rotor blade $B\ C_{max}$.

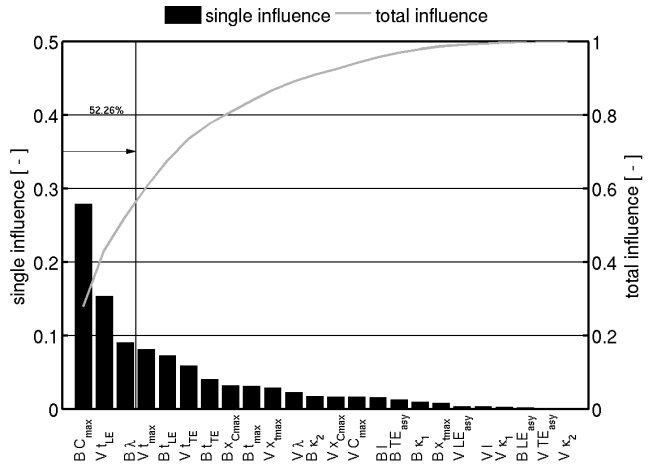


**Figure 3.** *Pareto* chart of isentropic efficiency $\eta_{is}$ at the rear stage

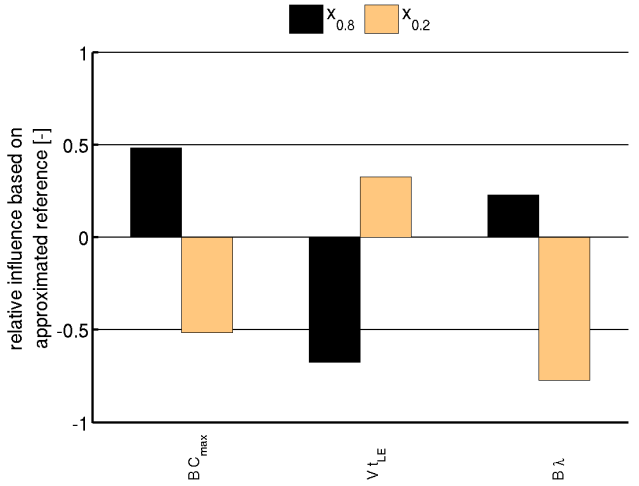


**Figure 4.** Sensitivities of $\eta_{is}$ to geometric changes at the rear stage

## Rear stage sensitivities

Similar analysis have been done for the rear stage. Fig. 3 illustrates the *Pareto* chart for the isentropic efficiency $\eta_{is}$ of the rear stage, analyzed at the reference mass flow. The three dominating geometric values are the max. camber of the rotor blade $B\ C_{max}$, the leading edge thickness of the stator vane $V\ t_{LE}$ and the stagger angle of the rotor blade $B\ \lambda$. Comparable to the front stage, the first three parameters have an accumulated impact about half of the overall changes caused by 24 geometric properties (The number of geometric properties is higher as at front stage because the rear stage has less correlations between the properties [3] [4]).

A detailed look to the three dominating geometric properties is given in Fig. 4. In contrast to the sensitivities of the front stage, the isentropic efficiency $\eta_{is}$ is decreasing with a decreased max. profile camber of the rotor blade $B\ C_{max}$. The changes caused by changing the leading edge thicknesses of the stator vane $V\ t_{LE}$ are similar to the front stage: decreasing the thickness results in an increased efficiency. Nevertheless, a strong dependency on the direction of the geometric change can be noticed. Increasing the leading edge thickness results in a stronger decrease in efficiency than decreasing the thickness about the same amount. Such a dependency can be seen for the stagger angle of the rotor blade $B\ \lambda$, too. Decreasing the stagger angle results in a steeper drop in efficiency compared to the efficiency gain of increased stagger angles (cf. [4]).

## Stage setups for full HPC calculations

In the following part of the paper, geometries are searched which show aerodynamic deviations to the reference airfoils as high as possible. Thereby, the geometric properties of the airfoils shall lay in between the range of the analyzed deteriorated ones. In doing so, the results of the previously done DoE's were used. Because there is no physical airfoil which is satisfying the desired requirements, the airfoils have to be generated by an in-house programmed algorithm [2]. As result, artificially deteriorated front and rear stages were generated and implemented into the full HPC model. To compare the aerodynamics of deteriorated front and rear stages to the reference geometry, all geometric properties were set to the mean values of the deteriorated airfoils [1]. Thereby, the leading edges of the front stage are getting thinner while the rear stage is tending towards thicker leading edges. Furthermore, the airfoils are opening and the stagger angles are decreased.

**Table 1.** Direction of geometric properties for max. $\eta_{is}$

| Geometric property | Front Stage | Rear Stage |
|---|---|---|
| $B\ t_{LE}$ | $\Downarrow$ | $\Uparrow$ |
| $V\ t_{LE}$ | $\Downarrow$ | $\Downarrow$ |
| $B\ \lambda$ | $\Downarrow$ | $\Uparrow$ |
| $V\ \lambda$ | $\Uparrow$ | $\Downarrow$ |
| $B\ C_{max}$ | $\Downarrow$ | $\Uparrow$ |
| $V\ C_{max}$ | $\Uparrow$ | $\Uparrow$ |

Moreover, to achieve aerodynamic deviations as wide as possible, stage setups for min. and max. isentropic efficiency were generated. Therefore, the previous shown aerodynamic sensitivities to geometric changes were used. Thus, the geometric properties which are mainly influencing the isentropic efficiency were - additionally to the mean value of the deteriorated airfoils - changed by $\pm\sigma$ in the direction for min. and max. efficiency. Table 1 shows the direction of chosen geometric properties for max. isentropic efficiency. As can be seen, the front stage setup for max. efficiency is characterized by decreased values of $B\ t_{LE}$, $V\ t_{LE}$, $B\ \lambda$ and $B\ C_{max}$. Whereas the values for $V\ \lambda$ and $V\ C_{max}$ are increased. The rear stage is characterized by decreased values of $V\ t_{LE}$ and $V\ \lambda$. The values for $B\ t_{LE}$, $B\ \lambda$, $B\ C_{max}$ and $V\ C_{max}$ are increased to achieve a rise in efficiency. The behavior for min. efficiency is vice versa.

After defining the values of the geometric airfoil properties, the airfoils are generated and meshed with an in-house programmed algorithm [2] and integrated into the full HPC CFD-model.

## CFD SETUP

The full HPC CFD-model contains all compressor rows, bleed-ports and cavities. Adjusting the integrated VSV-system, it is possible to simulate the entire compressor behavior to generate a compressor map. Nevertheless, for this studies just the throttle line for the operating condition cruise was simulated with the deteriorated front and rear stage. The behavior of the remaining parts of the compressor map was generated by scaling the reference map.

The CFD simulations have been carried out with the RANS solver *TRACE* [7] [8] [9] [10] from *DLR*. As already been mentioned, the operation point cruise was chosen for the generation of the deteriorated full HPC CFD-calculations. As inlet boundary condition the total pressure $p_{t25}$, total temperature $T_{t25}$, flow angle in circumferential direction $\alpha_{25}$, the radial distribution of the flow angle in radial direction $\beta_{25}(h/H)$, Mach Number $Ma_{25}$, turbulent intensity $Tu_{25}$ and turbulent length scale $TLM_{25}$ are chosen. As exit boundary condition, the averaged static pressure was chosen and varied to simulate the throttle line. Because the throttle lines are calculated as steady state condition, the last converged point is only representing a kind of numerical point of stall and not the physical. Further solver settings are summarized in Tab. 2.

**Table 2.** Boundary conditions

| Setting | Comment |
|---|---|
| $p_{t25}$, $T_{t25}$, $\alpha_{25}$, $\beta_{25}(h/H)$, $Ma_{25}$, $Tu_{25}$, $TLM_{25}$ | Extracted from streamline curvature calculations |
| Rotational speed | $n = n_{Cruise}$ |
| Walls | No slip walls (hydraulically smooth) |
| Blade to vane interface | Mixing plane |
| Turbulence model | Wilcox k-$\omega$ |
| Wall treatment | Wall functions |
| Stagnation point anomally fix | Kato Launder |
| Rotational effects | Bardina |
| Analysis type | Steady state |
| Blade / vane mesh | One pitch periodic |
| Dimensionless wall distance | $y^+_{Hub/Shroud} = 10$ $y^+_{Airfoil} = 3$ |

Subsequently to the simulations, the CFD results are analyzed for the isentropic efficiency $\eta_{is}$ and the total pressure ratio $\pi_{tt}$. The isentropic efficiency is calculated by the total pressure ratio:

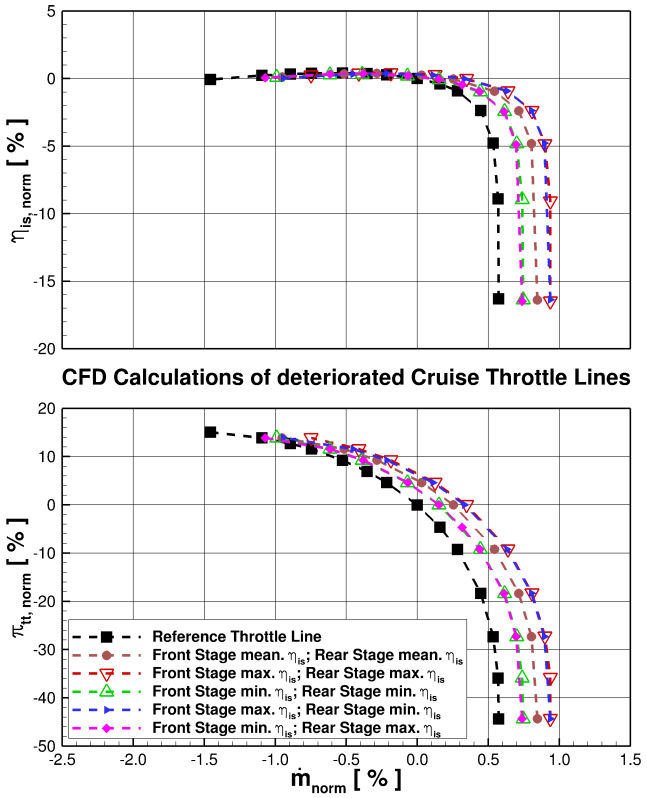


**Figure 5.** CFD-calculations of different deterioration combinations in the HPC

$$\pi_{tt} = \frac{p_{t3}}{p_{t25}} \tag{1}$$

and the total temperature ratio $\tau_{tt}$:

$$\tau_{tt} = \frac{T_{t3}}{T_{t25}} \tag{2}$$

with following equation:

$$\eta_{is} = \frac{\pi_{tt}^{\frac{\kappa-1}{\kappa}} - 1}{\tau_{tt} - 1} \tag{3}$$

The results of the deteriorated full HPC CFD-calculations are visualized in Fig. 5. Here, the reference throttle line for cruise condition is shown as well as different deterioration combinations of the front and rear stage. The lower part of the figure illustrates the normalized pressure ratio and the upper part the normalized isentropic efficiency. For the normalization the operating point of cruise was chosen. The throttle line of front and rear stage setups with all geometric properties set to the mean value of the statistical analysis of the deteriorated airfoils is shown as line with circle symbols. As can be seen, the throttle line is shifted towards higher massflows, which results for the reference mass flow in higher efficiency. Thereby, the shifting towards higher massflows

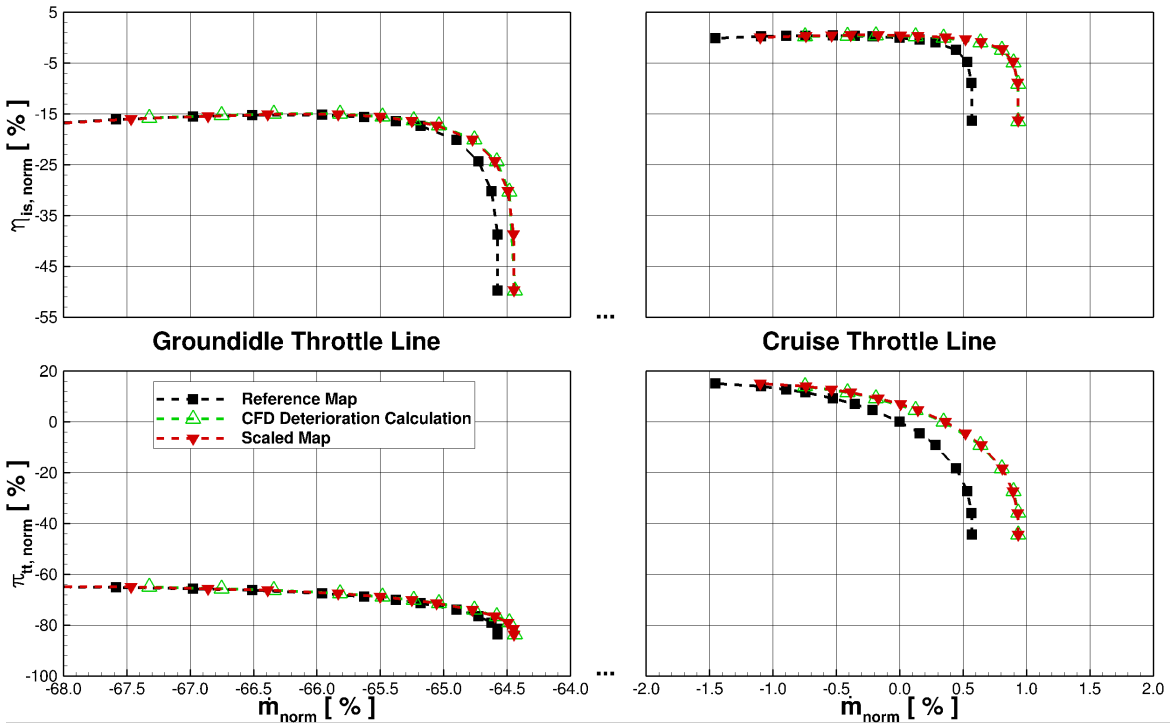


**Figure 6.** Validation of the HPC map scaling method

is mainly caused by decreased stagger angles of the deteriorated front blades. For the deterioration combination of max. $\eta_{is}$ in the front and rear stage, this effect is even strengthened (see. Tab. 1) and the shifting towards lower loadings is increasing. For the deterioration combination of min. $\eta_{is}$ this effect is weakened.

Another effect which is strengthening the increase in efficiency of the changed stage geometries is the influence of the leading edges. Because the modified airfoils have thinner leading edges, compared to the reference airfoils, the efficiency is increased (see Fig. 2 and 4). Nevertheless, it has to be mentioned that effects like increased gaps or roughness have not been taken into account.

Another observation is that the aerodynamic changes of the deteriorated HPC are mainly caused by the front stage. As can be seen, the throttle lines with the combination of max. $\eta_{is}$ in front and rear stage and the throttle line with max. $\eta_{is}$ in front and min. $\eta_{is}$ in the rear stage are overlapping. The same behavior can be observed for the combinations of min. $\eta_{is}$ in front and rear stage and the throttle line with min. $\eta_{is}$ in front and max. $\eta_{is}$ in the rear stage.

## COMPRESSOR MAP SCALING

Because it is not feasible to simulate a complete compressor map for each deterioration combination in the front and aft stage, a scaling of the reference compressor map was chosen. Therefore, scaling factors at the cruise condition point were generated by referencing the deteriorated operating point to the reference one [11]. Using this method, scaling factors for the massflow $\dot{m}$:

$$SF_{\dot{m}} = \frac{\dot{m}_{ADP}}{\dot{m}_{Ref,ADP}} \tag{4}$$

the total pressure ratio $\pi_{tt}$:

$$SF_{\pi_{tt}} = \frac{\pi_{tt,ADP}}{\pi_{tt,Ref,ADP}} \tag{5}$$

and the isentropic efficiency $\eta_{is}$:

$$SF_{\eta_{is}} = \frac{\eta_{is,ADP}}{\eta_{is,Ref,ADP}} \tag{6}$$

were generated. Afterwards, the reference compressor map parameters are multiplied with these scaling factors. As an example, Tab. 3 states the scaling factor values for the deterioration combination of max. $\eta_{is}$ in front and rear stage as well as for min. $\eta_{is}$ in both stages. Because of the shifting of the throttle lines towards higher mass flows (see Fig. 5), the scaling factor for the massflow $SF_{\dot{m}}$ is noticeably increased. In addition, the scaling factors for efficiency $SF_{\eta_{is}}$ and pressure ratio $SF_{\pi_{tt}}$ are slightly higher than 1.

**Table 3.** Values of used scaling factors

| Deterioration Combination | $SF_{\dot{m}}$ [ - ] | $SF_{\pi_{tt}}$ [ - ] | $SF_{\eta_{is}}$ [ - ] |
|---|---|---|---|
| FS & RS max $\eta_{is}$ | 1.00360 | 1.00026 | 1.00114 |
| FS & RS min $\eta_{is}$ | 1.00166 | 1.00017 | 1.00049 |

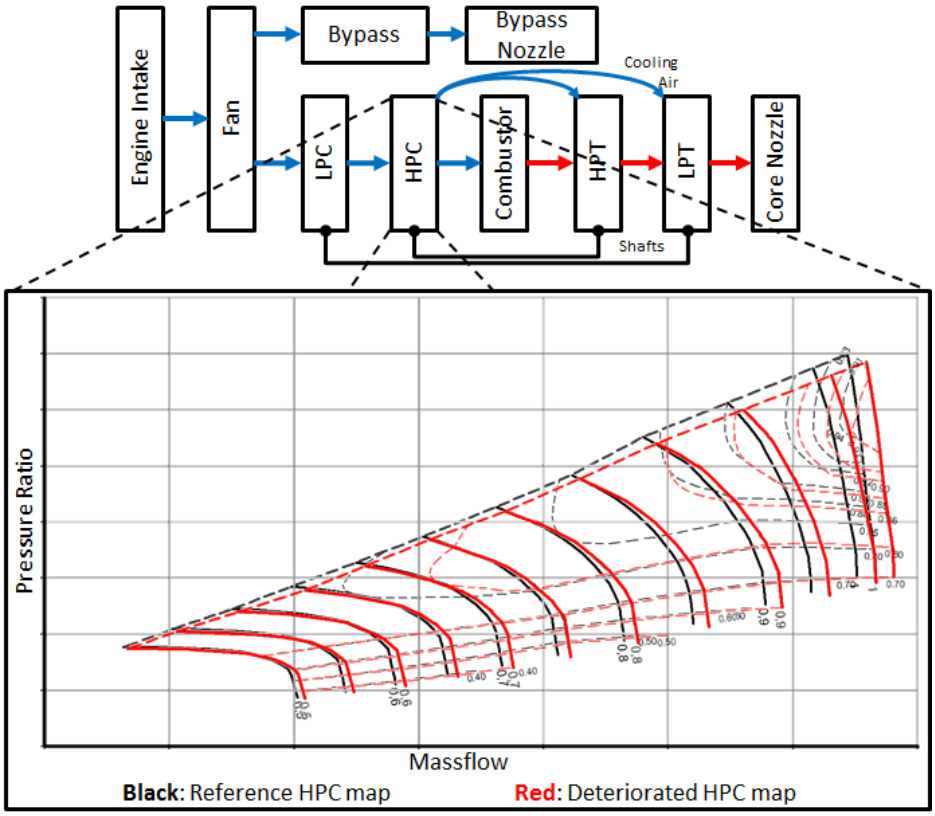


**Figure 7.** Scheme of a modular performance synthesis model with modified HPC maps

Because the scaling factors are only constants which are generated at the operating point of cruise, the functionality of the used method has to be validated. This was done by additional CFD-calculations at the left limit of the compressor map. This limit is represented by the throttle line with the rotational speed of the ground-idle operating point. To minimize the additional numerical effort, the validation is done for the deterioration level with the highest aerodynamic deviations to the reference throttle line of cruise. The chosen deterioration combination is max. $\eta_{is}$ in front and rear stage (see Fig. 5 and Tab. 3). Fig. 6 shows the sections for ground-idle and cruise of the compressor map. The reference map is characterized by the black, the CFD-calculations of the deteriorated compressor geometry by the green and the scaled compressor map by the red lines. Again, the lower part of the figure illustrates the normalized pressure ratio and the upper part the normalized isentropic efficiency. For the normalization the operating point of cruise was chosen, which has also been used for scaling the reference- to the deteriorated map. On the right hand side, a well agreement of the scaled to the CFD throttle line can be noticed. On the left hand side, the comparison for ground-idle is shown. As can be seen, the map scaling is working at the left limit of the map, too. Comparing the operating point on the ground-idle throttle line which is representing the ground-idle working point, the deviations between the CFD calculation and the scaled map have the following values:

- $\Delta\pi_{tt,\ Scaling\ to\ CFD}$ = -0.035 %
- $\Delta\dot{m}_{Scaling\ to\ CFD}$ = -0.056 %
- $\Delta\eta_{is,\ Scaling\ to\ CFD}$ = -0.018 %

As can be seen, the deviations between the CFD- and scaled throttle line are quite small and, therefore, negligible.

## MODULAR PERFORMANCE SYNTHESIS MODEL

To determine the changes of the engine performance due to changed HPC aerodynamics, a modular performance synthesis model of the analyzed jet engine was set up and validated by test cell data. For setting up the model, the software *GasTurb* [12] was used. The technique of modular performance synthesis is characterized by splitting up the thermodynamic cycle of a jet engine into its individual components (see Fig. 7 upper part). Thereby, the flow is calculated successively in each component independently from the other components. The component behavior can be described by simple equations (i.e. the pressure drop in a tube) or by complex component maps for the turbo-components (see Fig. 7 lower part).

**Table 4.** Changes of engine performance parameters for cruise condition

| Deterioration Combination | $\Delta\pi_{HPC}$ [ % ] to reference | $\Delta\eta_{HPC}$ [ % ] to reference | Δ SFC [ % ] to reference | Δ EGT [ K ] to reference | Δ BPR [ % ] to reference | $\Delta F_N$ [ % ] to reference |
|---|---|---|---|---|---|---|
| FS & RS max $\eta_{is}$ | +0.25 | +0.18 | -0.10 | -1.12 | -0.10 | -0.02 |
| FS & RS min $\eta_{is}$ | +0.12 | +0.08 | -0.04 | -0.52 | -0.04 | -0.01 |
| Generic min $\eta_{is}$ | -1.91 | -1.42 | +0.88 | +9.71 | +0.85 | +0.10 |

The modular performance synthesis is characterized by a 1D-calculation method, which is averaging the flow parameters like total pressure and temperature over the cross section. As a result, the modular performance synthesis is able to predict performance parameters like EGT or SFC.

In the modular performance synthesis model, the reference HPC map was replaced by the deteriorated ones (see Fig. 7 lower part) while leaving the rest of model in its original configuration. To prepare the scaled CFD maps, the software *Smooth C* was used [13]. With this software it is possible to inter- and extrapolate further throttle lines inside the compressor map and to transfer the data in a consistent input format for *GasTurb*.

## JET ENGINE PERFORMANCE CALCULATIONS

For evaluating the impact of modified stage geometries to the engine performance parameters, the HPC map of the modular performance synthesis model was replaced by the scaled ones. To guarantee an adjustment of the same engine operating condition despite the changed HPC maps, the model was regulated by the engine pressure ratio (EPR). This is the same engine control philosophy as for the real one. Afterwards, typical performance parameters are analyzed at the operating condition cruise. Table 4 summarizes chosen parameters, defining the compressor performance and the jet engine efficiency. As can be seen, the pressure ratio and efficiency of the HPC are increasing. This behavior can be explained by the scaling factors presented in Tab. 3. Again, it has to be mentioned, that because of the thinner leading edges in conjunction with an opening of the rows, the chosen geometric deterioration combinations result in a higher efficiency at the regarded massflow. Thereby, the higher scaling factors of the deterioration combination of max. $\eta_{is}$ in front and rear stage results in higher changes of $\pi_{HPC}$ and $\eta_{HPC}$, compared to the deterioration combination of min. $\eta_{is}$ in both stages. Although, just two compressor stages have been modified for the CFD-calculations, a noticeable effect on engine fuel economy can be observed: The given deterioration combinations are resulting in a 0.1% and 0.04% decreased SFC. Consequently, the EGT is decreased as well and the gain in EGT is about 1.12K and 0.52K.

Due to the small geometric changes, the deviations caused by the scaled HPC maps are quite small and are not representing the reality. As already mentioned, the airfoil gaps and roughness was not changed during this investigations. Especially these effects would result in a decreased compressor performance. Nevertheless, the process is able to reflect even these small changes in engine performance parameters like EGT and SFC, caused by small geometric changes inside only a few HPC rows.

To evaluate the impact of a strongly deteriorated HPC, a third HPC map modification was done. Therefore, all scaling factors are set to 0.98, which is a realistic range of deteriorated HPCs coming to a shop visit. Thereby, geometric variations of all HPC stages in conjunction with increased airfoil gaps and surface roughness are reducing the HPC performance. For such a HPC, the increase in SFC is about 0.88% and in EGT about 9.71K.

To give the reader a feeling for the provoked changes by the strongly deteriorated HPC, its impact to the fuel consumption of a typical civil flight mission is calculated. Thereby, the mission is characterized by taxiing on the ground followed by the take off and the succeeded cruise flight. Afterwards, the airplane is approaching and landing. With four hours, the operating condition of cruise is the longest flight period. For this magnitude of deterioration, the integrated fuel consumption of one engine is increased about 88.95kg which is an increase of 1.12%.

## CONCLUSIONS

In this paper, an evaluation of changes in jet engine performance caused by deteriorated HPCs was done. Therefore, a front and rear stage of the HPC were modified and the compressor performance was simulated by methods of CFD. In doing so, the results of two previously done DoEs were used to change the stage geometry in a manner for maximum and minimum efficiency. To lower the number of required numerical simulations, a compressor map scaling method was introduced and validated by an exemplary deterioration condition of the HPC. Using this scaling method, the calculation of just one deteriorated point on the throttle line would be sufficient to scale the complete reference map to a deteriorated one. Nevertheless, it was always the complete deteriorated throttle line calculated to evaluate its possible shape changes. Afterwards, the changed compressor maps were embedded in the modular performance synthesis model of the analyzed jet engine to evaluate its performance changes. The main results of the paper can be summarized as follows:

- Because deterioration leads to thinner airfoils, the efficiency shows a trend towards higher values. Additionally, the decreased stagger angle inside the front stage results in a throttle line shifting towards higher massflows. Nevertheless, it has to be mentioned that effects like increased gaps or roughness have not been taken into account.

- The investigated compressor behavior is mainly driven by the front stage. A HPC setup with an installed front and rear stage with max. efficiency shows nearly the same performance as an HPC setup with an installed front stage for max. efficiency and a rear stage with min. efficiency.

- The presented compressor map scaling method - which is working with constant multipliers for massflow, efficiency and pressure ratio respectively - is well working for the complete area of the map.

- Even just two stages of the HPC have been modified, a significant influence on jet engine performance was proven. Because of the already explained higher efficiency, the impact is positively. For the example of max. efficiency in front and rear stage, the SFC is decreasing about 0.1% and the EGT is approx. 1.1K colder.

- To show the impact of an overall deteriorated HPC, the scaling factors were all set to values representing an engine coming to the shop. For this example, a massive increase of the SFC was observed. Its value rises up about 0.9% and the EGT is 9.7K hotter. The increased SFC results in an increase of integrated mission fuel consumption (with a duration in cruise condition of 4h) about 89kg per engine which is 1.1% more than the reference value.

All in all, the presented process is able to reflect changes in engine performance parameters like EGT and SFC, caused by small geometric changes inside the HPC. Thus, the MRO would be able to evaluate the compressor performance at the incoming inspection and to identify sensitive compressor areas which provide a high potential to increase its performance.

In future, MRO companies would be able to classify serviceable airfoils with respect to their aerodynamics and impact to the HPC and jet engine performance. With the detailed knowledge of the varying airfoil aerodynamics, the HPC repair could be adjusted to given HPC efficiencies to meet the costumers requirements as cost-effective as possible. Furthermore, expensive troubleshooting because of failing the contracted engine performance could be avoided.

Nevertheless, further work has to be done. Additional compressor stages should be adjusted in their geometry to generate a fully changed HPC. Furthermore, the airfoils gaps and roughness could be increased to meet the true deteriorated compressor appearance.

## ACKNOWLEDGMENTS

The authors would like to thank MTU Maintenance Hannover GmbH for funding and for allowing the publication of this work.

## REFERENCES

[1] Marx, J., Städing, J., Reitz, G., and Friedrichs, J., 2013. "Investigation and Analysis of Deterioration in High Pressure Compressors". *DLRK Conference*.

[2] Reitz, G., and Friedrichs, J., 2016. "Procedure for Analyzing, Manipulating and Meshing of Compressor Blades to simulate their Flow". *International Journal of Gas Turbine, Propulsion and Power Systems (JGPP),* ***2016***(Volume 8).

[3] Reitz, G., Schlange, S., and Friedrichs, J., 2016. "Design of Experiments and Numerical Simulation of Deteriorated High Pressure Compressor Airfoils". *ASME GT2016-56024*.

[4] Reitz, G., Kellersmann, A., Schlange, S., and Friedrichs, J., 2016. "Comparison of Sensitivities to Geometrical Properties of Front and Aft High Pressure Compressor Stages". *DLRK 2016-420032*.

[5] Reitz, G., Dwinger, K., Schlange, S., Friedrichs, J., and Kappei, F., 2016. "Analysis of jet engine compressor deterioration and capturing correlations between geometric parameters". *ISROMAC 2016*.

[6] Lophaven, S. N., Nielsen, H. B., and Sondergaard, J., 2002. "DACE a Matlab Kriging toolbox; version 2; informatics and mathematical modelling". *Technical University of Denmark, Technical Report No. IMM-TR-2002-12*.

[7] Becker, K., Heitkamp, K., and Kügeler, E., 2010. "Recent Progress in a Hybrid-Grid CFD Solver for Turbomachinery Flows". *Proceedings of V. European Conference on Computational Fluid Dynamics*.

[8] Kügeler, E., 2004. "Numerisches Verfahren zur genauen Analyse der Kühleffektivität filmgekühlter Turbinenschaufeln". PhD thesis, Ruhr-Universität Bochum.

[9] Marciniak, V., Kügeler, E., and Franke, M., 2010. "Predicting Transition on Low-Pressure Turbine Profiles". *Proceedings of V. European Conference on Computational Fluid Dynamics*.

[10] Nürnberger, D., 01.01.2004. "Implizite Zeitintegration für die Simulation von Turbomaschinenströmungen". PhD thesis, Ruhr-Universität Bochum.

[11] Li, Y. G., Ghafir, M. F. A., Wang, L., Singh, R., Huang, K., and Feng, X., 2011. "Nonlinear Multiple Points Gas Turbine Off-Design Performance Adaptation Using a Genetic Algorithm". *Journal of Engineering for Gas Turbines and Power,* ***133***(7), p. 071701.

[12] GasTurb GmbH, 2015. *GasTurb 12: Design and Off-Design Performance of Gas Turbines*. Germany.

[13] GasTurb GmbH, 2015. *Smooth C 8.3: Preparing Compressor Maps for Gas Turbine Performance Modeling*. Germany.

## ABBREVIATIONS

| | |
|---|---|
| ADP | Aerodynamic Design Point |
| B | Blade |
| CFD | Computational Fluid Dynamics |
| DOC | Direct Operating Costs |
| DoE | Design of Experiment |
| EGT | Exhaust Gas Temperature |
| EM | Engine Manual |
| FS | Front Stage |
| HPC | High Pressure Compressor |
| LE | Leading Edge |
| MRO | Maintenance, Repair and Overhaul |
| RANS | Reynolds Averaged Navier Stokes |
| Ref | Reference |
| RS | Rear Stage |
| SF | Scaling Factor |
| TE | Trailing Edge |
| TKE | Turbulence Kinetic Energy |
| Tu | Turbulent Intensity |
| TLM | Turbulent Length Scale |
| TRACE | Turbomachinery Research Aerodynamics Computational Environment |
| SFC | Specific Fuel Consumption |
| V | Vane |

## NOMENCLATURE

**Latin Characters:**

| | |
|---|---|
| H | Absolute Duct Height |
| h | Height |
| k | Turbulence Kinetic Energy |
| Ma | Mach Number |
| n | Rotational Speed of N2 |
| p | Pressure |
| $p_t$ | Total Pressure |
| $T_t$ | Total Temperature |
| $y^+$ | Dimensionless Wall Distance |

**Greek Characters:**

| | |
|---|---|
| $\alpha$ | Absolute Circumferential Flow Angle |
| $\beta$ | Absolute Radial Flow Angle |
| $\eta_{is}$ | Isentropic Efficiency |
| $\kappa$ | Isentropic Exponent |
| $\sigma$ | Standard Deviation |
| $\tau_{tt}$ | Temperature Rise |
| $\omega$ | Dissipation Rate per Unit of TKE |

**Numbers:**

| | |
|---|---|
| 25 | HPC Inlet |
| 3 | HPC Outlet |

**Geometric Properties:**

| | |
|---|---|
| $c_{max}$ | Max. Profile Camber |
| l | Chord Length |
| $LE_{asy}$ | Leading Edge Asymmetry |
| $LE_{stretch}$ | Leading Edge Stretching |
| $r_{LE}$ | Leading Edge Radius |
| $r_{TE}$ | Trailing Edge Radius |
| $t_{LE}$ | Leading Edge Thickness |
| $t_{max}$ | Max. Profile Thickness |
| $t_{TE}$ | Trailing Edge Thickness |
| $TE_{asy}$ | Trailing Edge Asymmetry |
| $x_{c_{max}}$ | Position of max. Profile Camber |
| $x_{t_{max}}$ | Position of max. Profile Thickness |
| $\kappa_1$ | Metal Angle at Leading Edge |
| $\kappa_2$ | Metal Angle at Trailing Edge |
| $\lambda$ | Stagger Angle |